"New" reactive nitrogen chemistry reshapes the relationship of ozone to its precursors

Qinyi LI[1], Li ZHANG[1†], Tao WANG[1*], Zhe WANG[1], Xiao FU[1] and Qiang ZHANG[2]

(1) Department of Civil and Environmental Engineering, The Hong Kong Polytechnic University, Hong Kong, 999077, China; (2) Center for Earth System Science, Tsinghua University, Beijing, 100084, China

† Now at: Atmospheric and Oceanic Sciences Program, Princeton University, Princeton, New Jersey, 08544, United States; Geophysical Fluid Dynamics Laboratory, NOAA, Princeton, New Jersey, 08544, United States

*Corresponding author: Tao Wang (cetwang@polyu.edu.hk)

Abstract

Tropospheric ozone pollution has been a major environmental issue, and mitigation of this persistent problem requires a comprehensive understanding of the sensitivity of ozone to its precursors, i.e., nitrogen oxides (NO_x) and volatile organic compounds (VOCs). Recent studies have proposed several "new" reactive nitrogen chemical processes, including additional sources of nitrous acid, heterogeneous uptake of dinitrogen pentoxide, and production of nitryl chloride. These processes significantly affect the budgets of radicals and NO_x and hence the formation of ozone. In present study, we aim to investigate to what extent these processes alter the relationships between ozone and its precursors. A revised Weather Research and Forecasting model coupled with Chemistry incorporating the "new" nitrogen chemistry was adopted to simulate the ozone sensitivity regime in China in summer. The results showed that nitrogen chemistry changed the ozone sensitivity regime for approximately 40% of the simulated area with human influence, mostly from VOC-sensitive or NO_x-sensitive regimes to mixed-sensitive regime. The nitrogen chemistry changed the isopleth plots of the ozone peak values for major cities, suggesting a different strategy for controlling ozone pollution. This study underscores the need to consider unconventional nitrogen chemistry in air quality models used in the design of ozone control strategies.

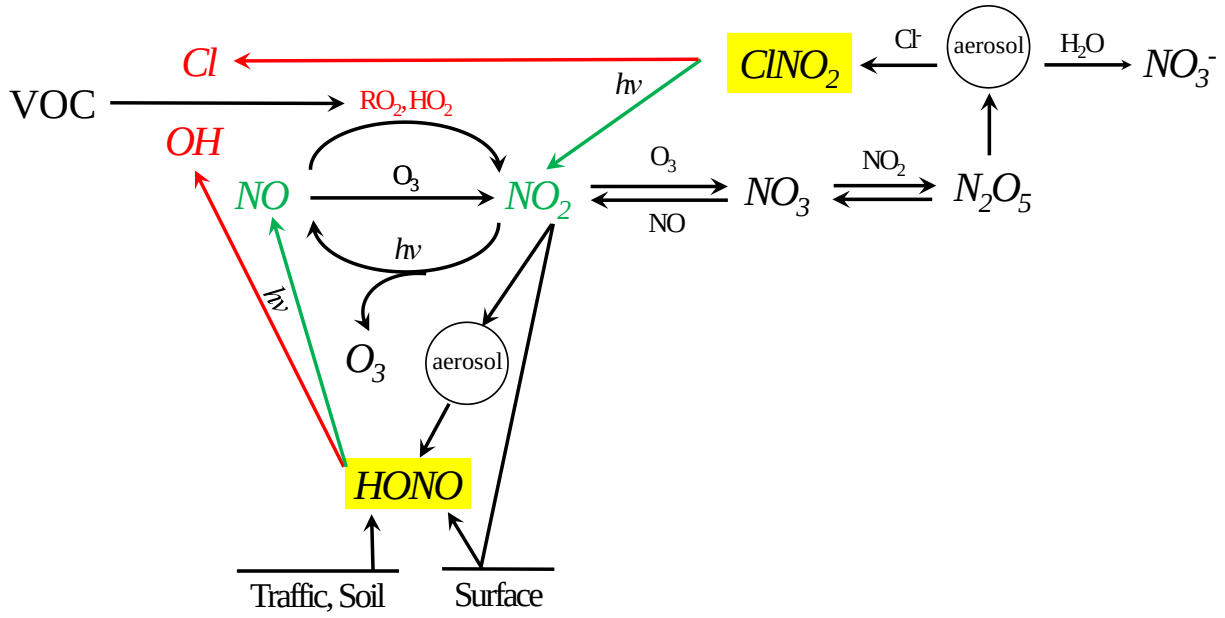

1. Introduction

Ozone (O_3) in the lower atmosphere has long been recognized as an air pollutant that adversely affects the health of human, the yields of crops, and the welfare of ecosystems.[1-3] In the troposphere, O_3 is formed by the photolysis of NO_2 (R1 and R2), and the formed O_3 then reacts with NO to produce NO_2 (R3). This cycle of NO_2–NO–O_3 is commonly referred to as the null cycle of O_3 formation, because it does not result in the net production or destruction of any O_3 molecules. In the presence of volatile organic compounds (VOCs), the hydroxyl (OH) radical initiates the degradation of the VOC to form the organic peroxy radical (RO_2) and hydroperoxy radical (HO_2), both of which transform NO into NO_2 without consuming O_3 (R4–R6), and the resulting NO_2 undergoes photolysis to generate O_3 (R1 and R2).[4]

$$NO_2 + h\nu \rightarrow NO + O^3P \quad (R1)$$

$$O^3P + O_2 \rightarrow O_3 \quad (R2)$$

$$NO + O_3 \rightarrow NO_2 + O_2 \quad (R3)$$

$$OH + VOC \rightarrow RO_2 + H_2O \quad (R4)$$

$$RO_2 + NO \rightarrow NO_2 + HO_2 + OVOC \quad (R5)$$

$$HO_2 + NO \rightarrow NO_2 + OH \quad (R6)$$

The scientific basis for controlling O_3 levels lies in the sensitivity of O_3 to the emission of its precursors (NO_x and VOCs). The relationship of O_3 to its precursors is determined by the source strength of RO_x radicals (the sum of OH, HO_2, and RO_2) relative to that of NO_x.[5-7] The sources of RO_x generally include the photolysis of O_3 (R7) and oxygenated VOCs (OVOCs), e.g., HCHO (R8), and the sinks of RO_x consist of the reaction of OH with NO_2 (R9) and the reactions between the peroxy radicals (R10 and R11). When the NO_x concentration is low, the RO_x level is largely controlled by the reactions between peroxy radicals and it is relatively insensitive to changing NO_x or VOC levels.[8] Under this condition, the production of O_3 is determined by the reactions of HO_2 and RO_2 with NO (R5 and R6) and it increases almost linearly with increasing NO_x emission. This condition is defined as the NO_x-sensitive regime and it is common in rural areas.[5] When the NO_x emission is high, the RO_x level is mainly controlled by the loss pathway via the reaction of OH with NO_2 (R9). An increase in NO_x emission results in a lower OH concentration and reduced production of RO_2 and O_3 locally. Under this condition, increased VOC levels lead to more VOCs reacting with OH and the higher production of RO_2 and O_3. Such a condition is defined as the VOC-sensitive regime and it often occurs in urban/industrial regions.[5] According to the above understanding of the underlying cause of the split between the VOC-sensitive and NO_x-sensitive regimes, any new emission source or atmospheric process that influences the relative abundance of radicals and NO_x could potentially affect the determination of the O_3 sensitivity classification and therefore the design of precursor control strategies.

$$O_3 + h\nu \rightarrow 2OH \quad \text{(R7)}$$

$$HCHO + h\nu \rightarrow 2HO_2 + CO \quad \text{(R8)}$$

$$OH + NO_2 \rightarrow HNO_3 \quad \text{(R9)}$$

$$HO_2 + HO_2 \rightarrow H_2O_2 + O_2 \quad \text{(R10)}$$

$$HO_2 + RO_2 \rightarrow ROOH + O_2 \quad \text{(R11)}$$

In the last decade, various sources of HONO, heterogeneous uptake of N_2O_5, and production of $ClNO_2$ have been reported, which have significant influences on the budgets of RO_x and NO_x.[9] The sources of HONO include direct emissions from traffic and soil and heterogeneous production on aerosol, ground, and ocean surfaces.[10-14] The direct emission of HONO from soil adds NO_x into the atmosphere. The formation of HONO by the heterogeneous processes reduces the NO_x levels (R12–R14). The photolysis of HONO is the predominant source of the OH radical in the polluted troposphere and also serves to recycle NO_x (R15).[15] The heterogeneous chemistry of N_2O_5 and

$ClNO_2$ consists of the heterogeneous uptake of N_2O_5 on the aerosol surface, production of $ClNO_2$, and photolysis of $ClNO_2$. The $N_2O_5/ClNO_2$ process acts as one of the major loss pathways of NO_x, one of the production source of HNO_3, and the dominant source of the chlorine (Cl) radical, which reacts with VOC as OH radical leading to the production of RO_x and O_3 (R16–R18).[16-19] This "new" nitrogen chemistry increases the RO_x sources and alters the fate of NO_x, thereby influencing the formation of O_3 and its sensitivity to the precursors.

$$2NO_2 + H_2O \rightarrow HONO + HNO_3 \quad (R12)$$

$$NO + HNO_3 \rightarrow HONO + NO_2 \quad (R13)$$

$$NO + NO_2 + H_2O \rightarrow 2HONO \quad (R14)$$

$$HONO + h\nu \rightarrow OH + NO \quad (R15)$$

$$N_2O_5 + H_2O + yCl^- \rightarrow (2-y)HNO_3 + yClNO_2 \quad (R16)$$

$$ClNO_2 + h\nu \rightarrow Cl + NO_2 \quad (R17)$$

$$Cl + VOC \rightarrow RO_2 + HCl \quad (R18)$$

Because of the nonlinear nature of O_3 chemistry, comprehensive mathematical tools, mainly chemical transport models (CTMs), have been used by the research community and regulatory agencies to investigate the O_3 sensitivity regime and establish control strategies. This pioneering research was initiated in the early 1990s in the U.S. by Sillman and co-workers, who used photochemical models to examine the sensitivity of O_3 concentrations to changes in the emissions of the precursors,[5, 20, 21] and similar research was later carried out in other parts of the world. Liang et al. evaluated the sensitivity of O_3 production in California using the Comprehensive Air Quality Modeling System with Extensions model (CAMx [22]).[23] Sillman and West conducted sensitivity simulations for Mexico City using the California Institute of Technology airshed model (CIT [24, 25]).[26] The Community Multiscale Air Quality modeling system (CMAQ) was used to evaluate the O_3 formation regime in China.[27] Wang et al. also used CMAQ (v4.5) to investigate the O_3 sensitivity in the Pearl River Delta (PRD).[28] Itahashi et al. used CMAQ (v4.7.1[13]) to study the O_3 sensitivity regime in East Asia.[29] Tie et al. applied the Weather Research and Forecasting model coupled with Chemistry (WRF-Chem v3 [30]) to evaluate the O_3 regime in Shanghai (in the Yangtze River Delta, YRD).[31]

The CTMs used in these previous O_3 sensitivity studies, except for CMAQ v4.7.1, only considered the gaseous formation of HONO from the OH+NO reaction, which is negligible compared with

the direct emission and the heterogeneous formation of HONO,[32] and the homogeneous hydrolysis of N_2O_5 with water vapor, which is negligible compared with the heterogeneous uptake of N_2O_5 on aerosol surfaces.[33] The CMAQ v4.7.1 model includes the heterogeneous uptake of N_2O_5 on aerosols to form nitrate, the heterogeneous formation of HONO on aerosol and ground surfaces, and the direct emission of HONO from traffic sources, but it does not consider the source of HONO from soils and oceans, the heterogeneous production of $ClNO_2$, or the gas-phase chemistry of the Cl radical with VOCs. Recent modeling studies have suggested significant influences of the additional HONO sources, $ClNO_2$ production, and subsequent Cl chemistry on the ambient concentrations of radicals and NO_x and the ozone production.[9, 32-36] It would be of great interest to explore whether and to what extent these "new" nitrogen chemical processes affect the simulations of ozone and precursor relationships and thereby the ozone precursor control strategies due to changes in the levels of radicals and NO_x.

In this study, we adopted an updated WRF-Chem model,[9] which incorporates all of the reported emissions/productions of HONO, the heterogeneous uptake of N_2O_5, the production of $ClNO_2$, and the gas-phase chlorine chemistry. The impact of the nitrogen chemistry on the levels of RO_x radicals and NO_x and the relationship of O_3 to its precursors were investigated. We then explored the implications of these results for the design of control strategies based on the isopleth of O_3 derived from the sensitivity simulations.

2. Model experiments

The original WRF-Chem (v3.6.1) and a revised version of WRF-Chem were utilized in this study. The original model includes the gaseous formation of HONO from OH and NO and the gaseous reaction between N_2O_5 and water vapor, but not the emission of HONO from traffic and soil, the heterogeneous formation of HONO from surfaces, the heterogeneous uptake of N_2O_5, subsequent production of HNO_3 and $ClNO_2$, nor the gas phase chlorine chemistry. The Reactive Nitrogen Oxides Mechanism (ReNOM), which considers the "new" chemistry of HONO and N_2O_5/$ClNO_2$, was implemented in the CBMZ_MOSAIC chemical module in WRF-Chem.[9] The incorporated HONO chemistry included the direct emissions of HONO from traffic exhaust and soil bacteria activity, and the heterogeneous production of HONO on ground, ocean, and aerosol surfaces, while the added N_2O_5/$ClNO_2$ chemistry consisted of the heterogeneous uptake of N_2O_5 on aerosol

surfaces, subsequent heterogeneous production of $ClNO_2$, photolysis of $ClNO_2$, and the gaseous reactions of the Cl radical and VOCs.[9] The revised model increases and has improved the prediction of O_3 in East China; the reader is referred to Zhang et al. for the details of the model development and validation.[9]

For this study, we followed Zhang et al. in the emission inventories of the routine air pollutants, the setting of domain, and the selection of the chemical and physical parameterizations, e.g., boundary layer scheme, land surface scheme, etc.[9] The emission inventories used in this study include the Multi-resolution Emission Inventory for China (MEIC; http://meicmodel.org/) from 2013 and the emission inventory for Asia (MIX; http://meicmodel.org/) from 2010, both of which have a resolution of 0.25° × 0.25°.[9] For the chlorine source, Zhang et al. used the Reactive Chlorine Emission Inventory (RCEI[37]), which was the only emission inventory available for East Asia at that time and was compiled for the year 1990 with a coarse resolution (1° × 1°).[9] For this study, we used an updated chlorine emission inventory for 2013 with a higher resolution (0.25° × 0.25°), and the reader is referred to supplement S2 for the details of this updated inventory. We adopted the parameterizations of dust emission and sea salt emission provided by the WRF-Chem model.[38] The simulations were run with one domain which has a horizontal resolution of 27 Km and 31 vertical layers with 8 layers within 1000 m above ground level. The relatively coarse grid resolution is adopted due to the spatial resolution of the emission inventory (0.25°, ~25 Km) and the large geophysical domain under study. The limitation of using such grid size is discussed in section 3.3. The final analysis data obtained from the National Centers for Environmental Predictions (NCEP) were used as the initial and boundary meteorological data (https://rda.ucar.edu/datasets/ds083.2/). The output from the Model for Ozone and Related Chemical Tracers model was used as the initial and boundary chemical data.[39]

The original WRF-Chem (Base) and the updated WRF-Chem (ReNOM) were run for one-month (July 2014) for the domain of East Asia with 100% NO_x and 100% anthropogenic VOC (AVOC) emissions, as shown in the emission matrix (the blue square in Fig. S1). The differences in the RO_x and NO_x levels between the Base and ReNOM cases represent the effect of the nitrogen chemistry on these species, as discussed in Section 3.1. Sensitivity runs were then conducted using the Base and ReNOM models over the same period by reducing the AVOC or NO_x emissions by 50%, as suggested by Sillman and West and shown in the emission scenarios matrix (the red triangles in

Fig. S1).[26] The Base, Base-50%NO_x, and Base-50%AVOC cases were used to determine the sensitivity of O_3 production with the original model. The differences between O_3 in the ReNOM and ReNOM-50%NO_x or ReNOM-50%AVOC cases were used to assess the O_3 sensitivity using the revised WRF-Chem model. The results are shown in Section 3.2.

To investigate whether the inclusion of the aforementioned chemical processes significantly changed the ozone isopleth for the major cities of China, sensitivity simulations were undertaken with the Base and ReNOM models for three days (July 28–30, 2014; during which the O_3 concentrations were elevated in East China) by reducing the NO_x and/or AVOC emissions by 0%, 25%, 50%, 75%, or 100% (in total 25 cases), as depicted in the emission scenarios (the black crosses in Fig. S1). The peak O_3 concentrations for the large cities in the North China Plain (NCP) and YRD, including Beijing (BJ), Tianjin (TJ), Shijiazhuang (SJZ), Jinan (JN), Zhengzhou (ZZ), Hefei (HF), Nanjing (NJ), and Shanghai (SH), were used to generate the O_3 isopleth figure, which was applied to design the O_3 control strategy (Section 3.3).

3. Results and discussion

3.1 Simulation of HONO and $ClNO_2$ and their effects on RO_x and NO_x

The simulation based on WRF-Chem with the "new" nitrogen chemistry (ReNOM case) showed elevated concentrations of HONO (average of 1h daily maximum > 1 ppb) at the surface over the five city clusters (NCP, YRD, PRD, central China (CC), and the Sichuan Basin (SCB)), as shown in Fig. 1a. The simulated $ClNO_2$ concentrations were concentrated over the NCP, YRD, CC, and SCB (average of 1h daily maximum > 0.3 ppb) at ground level (Fig. 1b). The simulated $ClNO_2$ level was at low level in another urban cluster, PRD, whereas the highest $ClNO_2$ level was observed in the PRD region in the winter of 2013,[40] which is probably due to the seasonal difference in meteorological conditions (summer and winter) as suggested by Zhang et al.[9] The HONO level simulated using the Base case was negligible (data not shown), and there was no $ClNO_2$ in the Base case. The use of the ReNOM model indicated significantly higher levels of HONO and $ClNO_2$.

The addition of the HONO and N_2O_5/$ClNO_2$ chemistry substantially changed the simulated photochemical characteristics over East Asia. The simulated daytime-averaged levels of RO_x

radicals increased across the domain mostly by 2-10 ppt and with a maximum increase of 20.5 ppt (~54.9%) for the ReNOM case compared with the Base case (Fig. 2a and b), due to the increased sources of radicals in ReNOM case. The areas with significant increases in the RO_x levels were mostly over the city clusters, especially the NCP and YRD, because the increases in the HONO and $ClNO_2$ levels were mostly over urban areas, particularly in these two clusters. The simulated NO_x concentrations were generally 2-5 ppb and with a maximum of 12.7 ppb (~15.3%) lower in most of the region in the ReNOM case (Fig. 2c and d), mainly because the N_2O_5/$ClNO_2$ chemistry reduces the NO_x level. The photolysis of HONO and $ClNO_2$ recycled the NO/NO_2 and hence partially offset the removal of the NO_x. The impact of the HONO and N_2O_5/$ClNO_2$ chemistry on the RO_x and NO_x levels in the PRD was smaller compared with that in the NCP and YRD, because the simulated HONO and $ClNO_2$ concentrations were lower in the PRD during summer.

3.2 Impact of the nitrogen chemistry on the determination of O_3 sensitivity

The effect of the nitrogen chemistry on the O_3 sensitivity to its precursors can be determined by comparing the differences in O_3 concentrations between the simulations with the original emissions and the simulations with reduced NO_x/AVOC emissions.[26] The changes in the simulated O_3 concentrations due to the reduced NO_x/AVOC emissions are shown in Fig. 3, in which we used the daytime-averaged O_3 concentrations (10:00–17:00, local time). For the Base case, the reduced NO_x level led to an O_3 increase over urban areas and a decrease in rural regions with no significant changes observed over remote areas and ocean (Fig. 3b). The reduced AVOC emissions resulted in decreased O_3 levels, mostly over urban areas (Fig. 3c). The pattern of O_3 changes was reshaped in the ReNOM case (Fig. 3e and f). In particular, the region with the O_3 increase due to the NO_x reduction significantly shrunk in the NCP and YRD and modestly altered in the PRD.

To quantitatively evaluate the effect of the nitrogen chemistry on the O_3 sensitivity, the definitions of O_3 sensitivity regimes proposed by Sillman and West were adopted, namely, NO_x-sensitive, VOC-sensitive, mixed-sensitive, NO_x-titration, and no sensitivity.[26] Briefly, a location is defined as NO_x-sensitive region (VOC-sensitive region) where the O_3 change in response to reduced NO_x (VOC) emission is larger than that to reduced VOC (NO_x) emission, while a place is regarded as mixed-sensitive region if the O_3 change due to reduced NO_x and VOC emission are comparable. Please see the supplement S3 for the details of these definitions. The determined O_3 sensitivity regime in East Asia in the Base case is shown in Fig. 4a and Table 1. The majority of the area

(mostly remote regions and ocean) in the modeling domain showed no sensitivity to the precursor emissions in the Base case. For the grids influenced by the anthropogenic emissions, the NO_x-sensitive grids dominated the rural areas, whereas the urban areas (where the NO_x concentration is elevated in Fig. 2c) were mostly determined to be VOC-sensitive, and the suburban regions were diagnosed as mixed-sensitive regions. The NO_x-sensitive grids accounted for 63.1% of the areas with intense human influence, whereas the proportions of mixed- and VOC-sensitive grids were 16.9% and 19.7%, respectively, and the NO_x-titration regime only appeared in a few grids. The simulated O_3 regime simulated in the Base case is consistent with the previous studies, which used the model without the comprehensive nitrogen chemistry. Liu et al. used the CMAQ model to study the O_3 sensitivity through emission reduction sensitivity runs and suggested the occurrence of VOC-sensitive characteristics in the urban areas and NO_x-sensitive characteristics in other regions in China.[27] Li et al. also applied CMAQ to study the O_3 formation regime in the YRD and concluded that the urban area of Shanghai was a VOC-sensitive region whereas the rural area was a NO_x-sensitive region.[41] Furthermore, Tie et al. reported a strong VOC-sensitive regime for Shanghai and its surrounding region based on simulations using the WRF-Chem model.[31] Wang et al. performed sensitivity studies of O_3 formation for the PRD using the CMAQ, and the results suggested VOC-sensitive features in the central PRD and NO_x-sensitive characteristics in the southwestern PRD.[28]

The addition of the HONO and N_2O_5/$ClNO_2$ chemistry showed some effects on the O_3 sensitivity regime in East Asia (Fig. 4b and Table 1). The percentages of NO_x-sensitive and VOC-sensitive regions dropped to 57.6% (from 63.1%) and 17.2% (19.7%), respectively, while that of mixed-sensitive regions increased considerably to 24.9% (from 16.9%), compared with the results from the Base case. The grids assigned as the NO_x-titration regime remained negligible in the ReNOM case. In the urban areas, the sensitivity of O_3 to the emissions of its precursors was mostly VOC-sensitive in the Base case, but a significant portion changed to the mixed-sensitive regime after considering the nitrogen chemistry. These changes were due to (1) the increased levels of radicals in the urban atmosphere and hence the increased levels of VOC oxidation, and (2) the reduced levels of NO_x and hence a decrease in the NO_x titration effect. In the regions where high levels of non-anthropogenic (soil and ocean) sources of HONO were simulated, the grid changed from the NO_x-sensitive regime in the Base case to the mixed-sensitive (coastal regions), VOC-sensitive (urban Japan), or no sensitivity (rural Taiwan and Japan) regimes. This result was probably due to

the additional HONO increasing the NO levels in the atmosphere, which reduces the dependence of O_3 formation on the NO_x level. Overall, the consideration of the HONO and N_2O_5/$ClNO_2$ chemistry led to changes in the simulated O_3 sensitivity for approximately 40% of the areas influenced by anthropogenic emissions, and an increase of the areas in the mixed-sensitive regime.

3.3 Implications for ozone control strategies

Here we conducted 50 sensitivity simulations with the original and updated WRF-Chem models by reducing the NO_x and/or AVOC emissions by 0%, 25%, 50%, 75%, or 100% for July 28–30, 2014, during which the O_3 levels in East China were elevated, with average simulation of daily maximum O_3 concentrations in the NCP and YRD of 145.6 ppb and 108.3 ppb, respectively. The isopleths of the average daily maximum values of O_3 concentrations from the 50 sensitivity runs with the Base and ReNOM models are shown in Fig. 5 for eight major cities in the regions where the nitrogen chemistry showed a strong influence during the simulation period, i.e., the NCP and YRD, including BJ, TJ, SJZ, JN, ZZ, HF, NJ, and SH. We used 9 grids (3x3 grids, i.e. 81x81Km^2) to represent each city. The general locations of these cities were shown in Fig 4.

For the Base case, the simulated O_3 values with 100% NO_x and 100% AVOC emissions for six out of the eight cities, except for ZZ and HF, were above the ridge line (i.e., strong VOC-sensitive). If only NO_x control is implemented, these six cities would be expected to experience an increase of O_3, the so-called "NO_x disbenefit", before the decrease of O_3 (Fig. 5), highlighting the nonlinear relationship of O_3 production and NO_x emission in urban areas. If only the AVOC emission is reduced, the peak values of O_3 concentrations in the urban areas would be reduced, but the overall production of O_3, which is determined by the NO_x emission, would remain the same.[5] An effective strategy in these regions would be to implement NO_x and AVOC control in parallel, and the NO_x:AVOC reduction ratio should be designed according to the O_3 isopleth to avoid the negative effects of NO_x reduction.[42]

For the ReNOM case, the pattern of the O_3 isopleth was clearly altered upon considering the additional nitrogen chemistry. The O_3 concentrations with 100% NO_x and AVOC emissions were mostly on or near the ridge line (i.e., mixed- or slightly VOC-sensitive). Seven out of the eight cities (except for SH) would not experience the NO_x disbenefit with the reduction of NO_x, suggesting that the negative effect of NO_x reduction is lower than previously predicted without the

new nitrogen chemistry. Moreover, reductions in either NO_x or AVOC emissions would decrease the O_3 levels in these cities in the NCP and YRD, which permits more flexibility when designing the control strategies. Our result from the comprehensive model is supported by a previous observation-based study in Beijing, which indicated a transition (mixed-sensitive) regime based on field measurements and box model calculations at an urban site.[43] Therefore, we conclude that consideration of the new chemical processes would not only improve air quality models for simulating the budgets of radicals and NO_x and the production of ozone[9] but may also alter the simulated sensitivity of ozone to its precursors and thereby have important implications for the design of O_3 control strategies. One such implication, as demonstrated by the simulation of one summer episode in the present study, is that controlling NO_x may be more effective than previously thought for mitigating O_3 pollution in urban areas of East China. Apart from alleviating O_3 pollution, reducing NO_x emissions will also decrease NO_2 and nitrate aerosol, of which the latter is an important contributor to $PM_{2.5}$ levels in many cities in East China.[44-47]

The present work focuses on China and on a summer season. More studies are needed on the effects of controlling NO_x emissions in different regions and seasons, and to this end we recommend that air quality models should include the newly reported nitrogen chemical processes. Our study adopted a relatively coarse grid resolution (27Km), in view of a large region of study and access to an emission inventory of 0.25 degree resolution. A previous modeling study, Cohan et al., has shown some dependence of O_3 sensitivity on the grid resolution and that with finer resolution, the NOx emission is more intense in the grids with large NOx sources, e.g. urban or industrial regions, and the O_3 formation is more limited by the AVOC in these grids.[48] If an emission inventory of higher resolution were available for our study, the O_3 formation would be more limited by AVOC in the domain with finer grids than that with coarser grids. The HONO level in the finer grids would be higher than that in coarse grids, considering that the direct emission and heterogeneous production of HONO on surfaces would be more intense with higher NOx emission. Therefore, the influence of nitrogen chemistry on O_3 sensitivity in urban/industrial regions would likely be larger in the domain with finer grids compared to what is observed in the present work, and more urban/industrial areas would become mixed- or NOx-sensitive regimes. It would be of great interest to perform simulations with finer resolution emission inventories in future research.

312 Table 1. The areas (model grids) and the proportions of the O_3 sensitivity regimes in East Asia[a]

	Base		ReNOM	
	grid (27*27 km^2)	percentage	grid (27*27 km^2)	percentage
NO_x-sensitive	4363	63.1%	3647	57.6%
mixed-sensitive	1171	16.9%	1577	24.9%
VOC-sensitive	1359	19.7%	1087	17.2%
NO_x-titration	18	0.26%	22	0.35%

313 a. Note that this table excludes the model grids with no-sensitivity which account for 21144 grids and 21722
314 grids for Base and ReNOM cases, respectively.

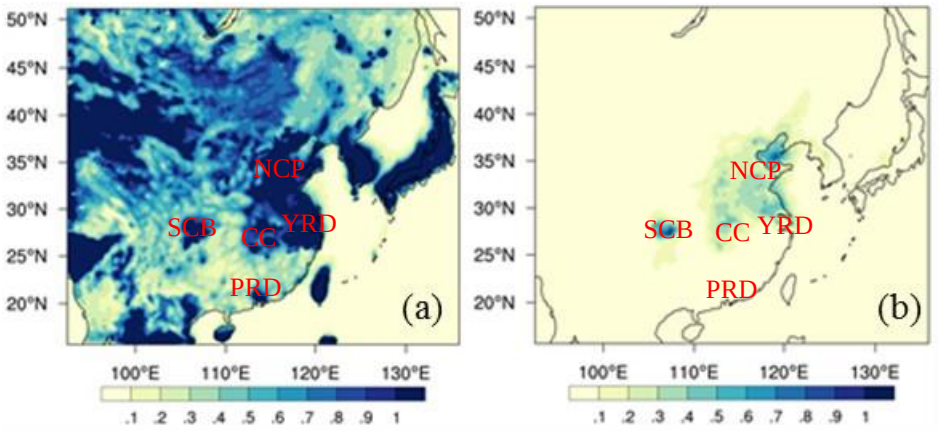

315

316 Fig. 1. Average of 1h daily maximum concentrations of (a) HONO (ppb) and (b) $ClNO_2$ (ppb) at ground
317 level simulated using the ReNOM model with 100% NO_x and AVOC emissions for July 2014.

318

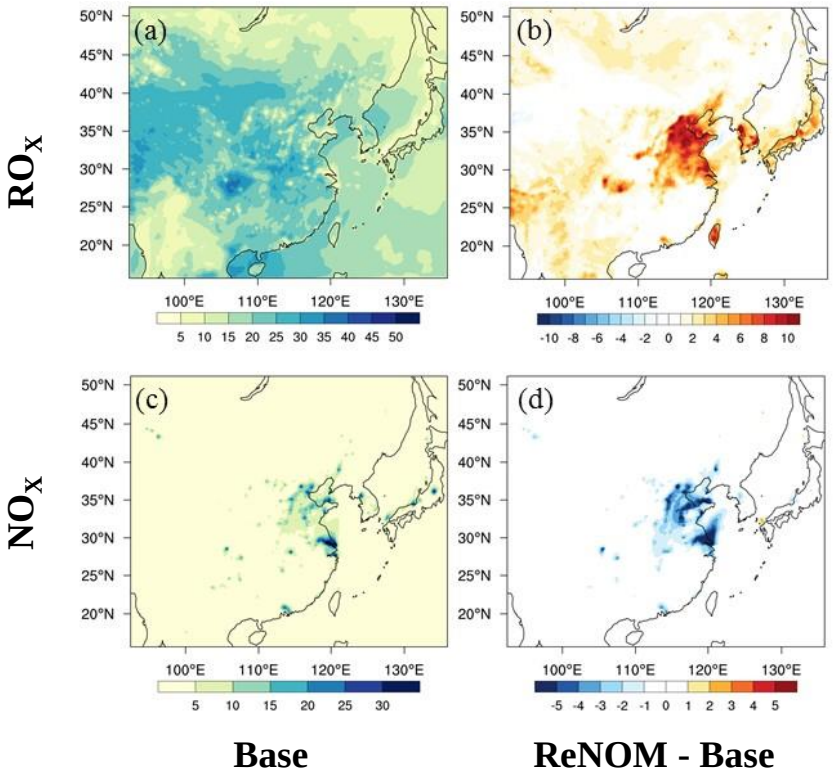

Fig. 2. The daytime average (10:00–17:00) concentrations of (a) RO_x radicals (ppt) and (c) NO_x (ppb) using the Base model, and the impacts of nitrogen chemistry on the (b) RO_x radicals (ppt) and (d) NO_x (ppb) for July 2014.

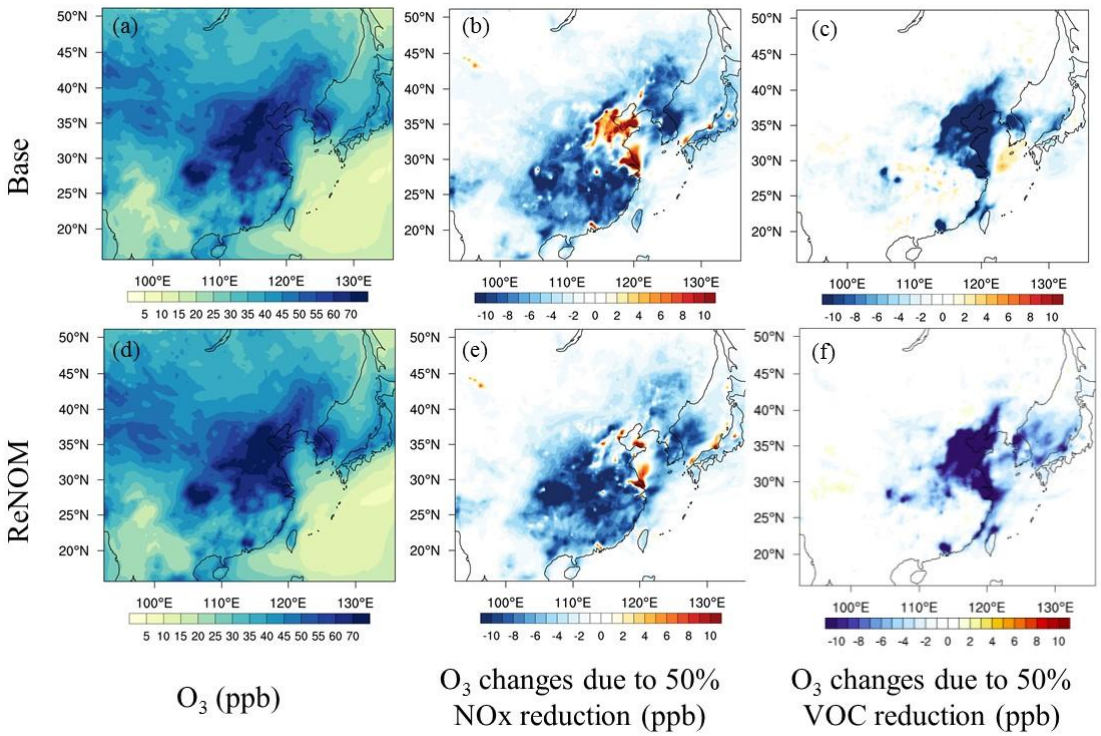

323

324 Fig. 3. Simulated daytime average O_3 in July 2014 using the (a) Base and (d) ReNOM models; the changes
325 in the O_3 levels upon a 50% reduction in the NO_x levels in the (b) Base and (e) ReNOM models; and the
326 changes in the O_3 levels upon a 50% reduction in the VOC levels in the (c) Base and (f) ReNOM models.

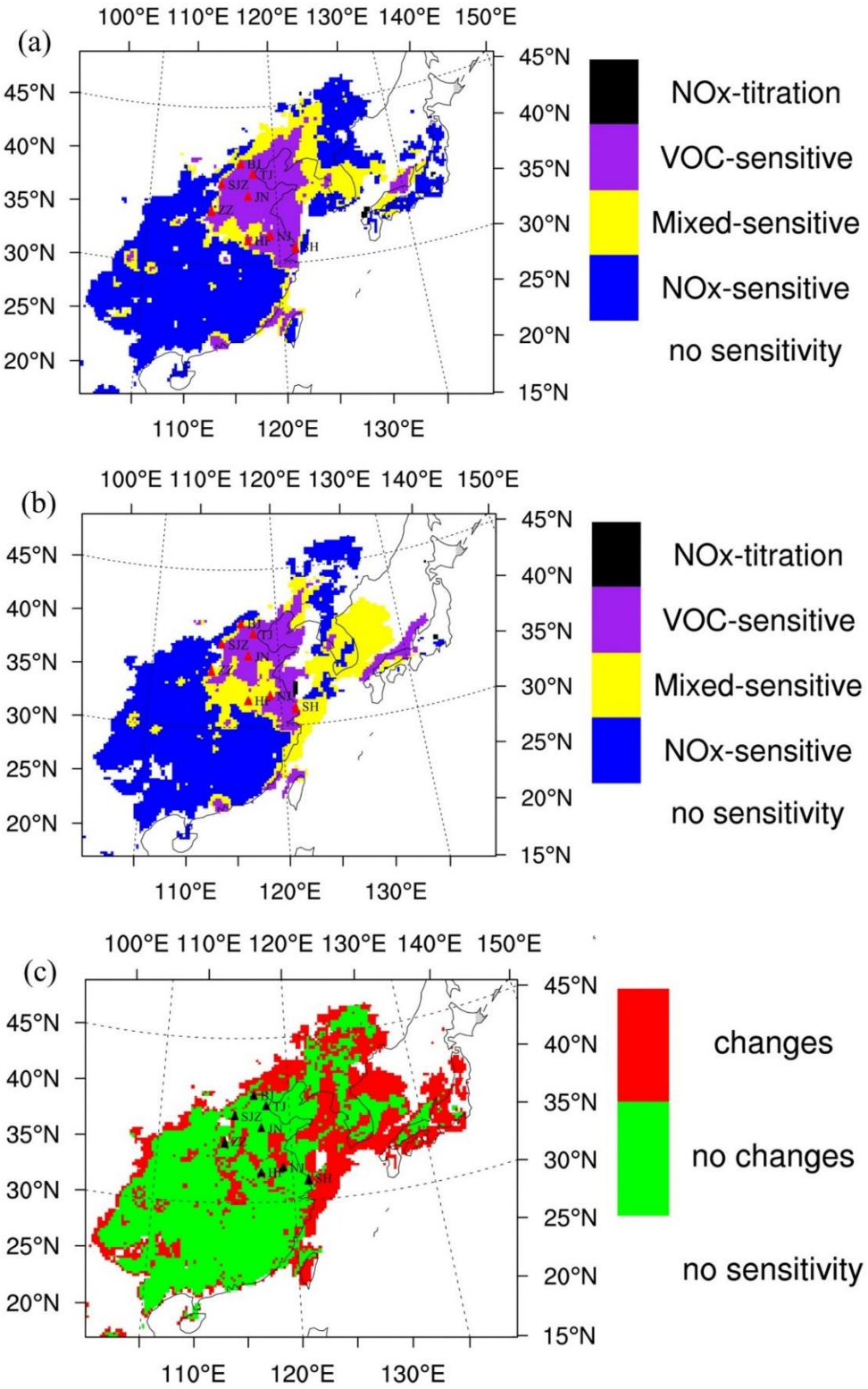

Fig. 4. The determined O_3 sensitivity regimes for East Asia using the (a) Base and (b) ReNOM models, and (c) the changes in simulated O_3 sensitivity for this region upon considering the nitrogen chemistry. The triangles represent the locations of the eight major cities in the NCP and YRD.

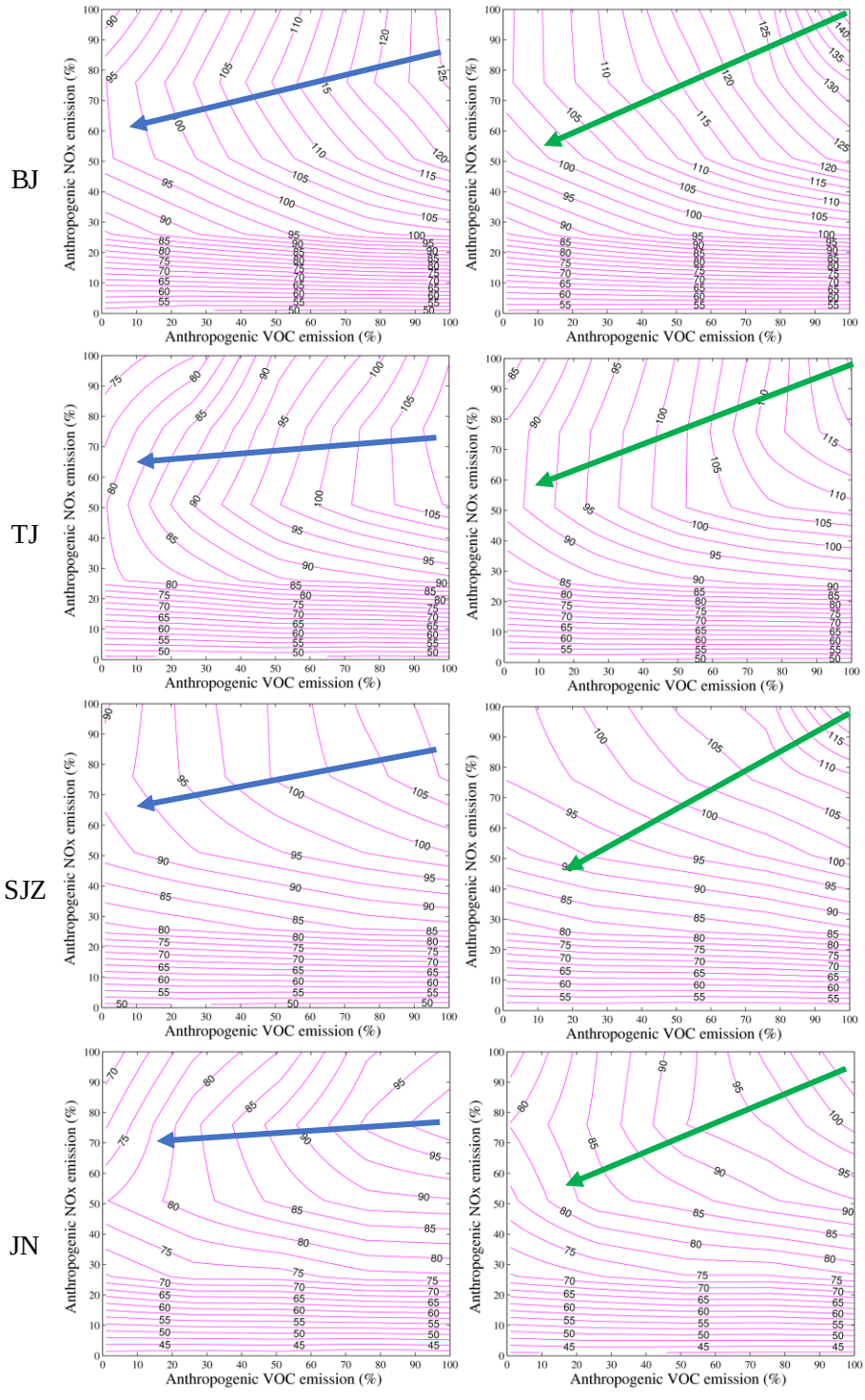

Fig. 5. The simulated isopleth of peak O_3 concentrations for BJ, TJ, SJZ, JN, ZZ, HF, NJ, and SH using the Base and ReNOM models. The blue and green lines represent the ridge lines of the isopleth.

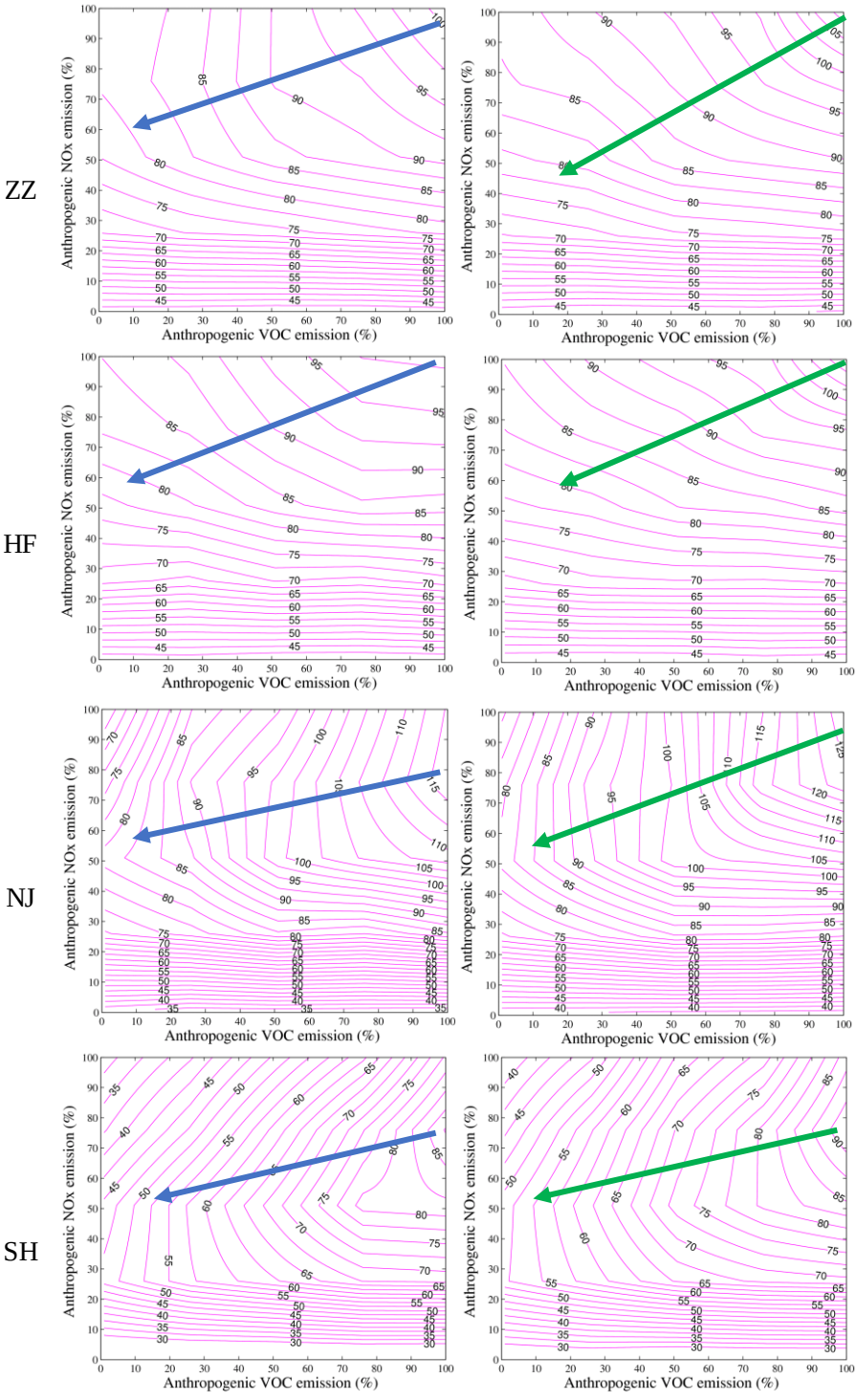

Fig 5. Continued.

Acknowledgement

This study is supported by a Hong Kong Polytechnic University PhD studentship, the Collaborative Research Fund of the Hong Kong Research Grants Council (C5022-14G), and the National Natural Science Foundation of China (91544213).

Supporting Information Available

Emission matrix for WRF-Chem simulation, updated chlorine inventory in China, and definitions of the O_3 sensitivity regimes.

Reference

1. WHO *Air Quality Guidelines. Global update 2005*; World Health Organization: 2006.

2. Lefohn, A. S.; Malley, C. S.; Simon, H.; Wells, B.; Xu, X.; Zhang, L.; Wang, T., Responses of human health and vegetation exposure metrics to changes in ozone concentration distributions in the European Union, United States, and China. *Atmospheric Environment* **2017,** *152*, 123-145.

3. Fowler, D.; Cape, N. J.; Coyle, M.; Flechard, C.; Kuylenstierna, J.; Hicks, K.; Derwent, D.; Johnson, C.; Stevenson, D., The Global Exposure of Forests to Air Pollutants. *Water, Air, & Soil Pollution* **1999,** *116*, (1/2), 5-32.

4. Atkinson, R., Atmospheric chemistry of VOCs and NO x. *Atmospheric environment* **2000,** *34*, (12), 2063-2101.

5. Sillman, S., The relation between ozone, NO x and hydrocarbons in urban and polluted rural environments. *Atmospheric Environment* **1999,** *33*, (12), 1821-1845.

6. Kleinman, L. I., Seasonal dependence of boundary layer peroxide concentration: The low and high NO x regimes. *Journal of Geophysical Research: Atmospheres* **1991,** *96*, (D11), 20721-20733.

7. Kleinman, L. I., Low and high NOx tropospheric photochemistry. *Journal of Geophysical Research: Atmospheres* **1994,** *99*, (D8), 16831-16838.

8. Sillman, S.; He, D., Some theoretical results concerning O3 - NOx - VOC chemistry and NOx - VOC indicators. *Journal of Geophysical Research: Atmospheres* **2002,** *107*, (D22).

9. Zhang, L.; Li, Q.; Wang, T.; Ahmadov, R.; Zhang, Q.; Li, M.; Lv, M., Combined impacts of nitrous acid and nitryl chloride on lower-tropospheric ozone: new module development in WRF-Chem and application to China. *Atmospheric Chemistry and Physics* **2017,** *17*, (16), 9733-9750.

10. Gutzwiller, L.; Arens, F.; Baltensperger, U.; Gäggeler, H. W.; Ammann, M., Significance of Semivolatile Diesel Exhaust Organics for Secondary HONO Formation. *Environmental Science & Technology* **2002,** *36*, (4), 677-682.

11. Su, H.; Cheng, Y.; Oswald, R.; Behrendt, T.; Trebs, I.; Meixner, F. X.; Andreae, M. O.; Cheng, P.; Zhang, Y.; Pöschl, U., Soil Nitrite as a Source of Atmospheric HONO and OH Radicals. *Science* **2011,** *333*, (6049), 1616-1618.

12. Zha, Q.; Xue, L.; Wang, T.; Xu, Z.; Yeung, C.; Louie, P. K. K.; Luk, C. W. Y., Large conversion rates of NO2 to HNO2 observed in air masses from the South China Sea: Evidence of strong production at sea surface? *Geophysical Research Letters* **2014,** *41*, (21), 7710-7715.

13. Foley, K. M.; Roselle, S. J.; Appel, K. W.; Bhave, P. V.; Pleim, J. E.; Otte, T. L.; Mathur, R.; Sarwar, G.; Young, J. O.; Gilliam, R. C.; Nolte, C. G.; Kelly, J. T.; Gilliland, A. B.; Bash, J. O., Incremental testing of the Community Multiscale Air Quality (CMAQ) modeling system version 4.7. *Geoscientific Model Development* **2010,** *3*, (1), 205-226.

14. Li, G.; Lei, W.; Zavala, M.; Volkamer, R.; Dusanter, S.; Stevens, P.; Molina, L. T., Impacts of HONO sources on the photochemistry in Mexico City during the MCMA-2006/MILAGO Campaign. *Atmospheric Chemistry and Physics* **2010,** *10*, (14), 6551-6567.

15. Kleffmann, J., Daytime sources of nitrous acid (HONO) in the atmospheric boundary layer. *ChemPhysChem* **2007,** *8*, (8), 1137-1144.

16. Brown, S. S.; Ryerson, T. B.; Wollny, A. G.; Brock, C. A.; Peltier, R.; Sullivan, A. P.; Weber, R. J.; Dubé, W. P.; Trainer, M.; Meagher, J. F.; Fehsenfeld, F. C.; Ravishankara, A. R., Variability in Nocturnal Nitrogen Oxide Processing and Its Role in Regional Air Quality. *Science* **2006,** *311*, (5757), 67-70.

17. Osthoff, H. D.; Roberts, J. M.; Ravishankara, A. R.; Williams, E. J.; Lerner, B. M.; Sommariva, R.; Bates, T. S.; Coffman, D.; Quinn, P. K.; Dibb, J. E.; Stark, H.; Burkholder, J. B.; Talukdar, R. K.; Meagher, J.; Fehsenfeld, F. C.; Brown, S. S., High levels of nitryl chloride in the polluted subtropical marine boundary layer. *Nature Geoscience* **2008,** *1*, (5), 324-328.

18. Thornton, J. A.; Kercher, J. P.; Riedel, T. P.; Wagner, N. L.; Cozic, J.; Holloway, J. S.; Dubé, W. P.; Wolfe, G. M.; Quinn, P. K.; Middlebrook, A. M.; Alexander, B.; Brown, S. S., A large atomic chlorine source inferred from mid-continental reactive nitrogen chemistry. *Nature* **2010,** *464*, (7286), 271-274.

19. Simon, H.; Kimura, Y.; McGaughey, G.; Allen, D. T.; Brown, S. S.; Coffman, D.; Dibb, J.; Osthoff, H. D.; Quinn, P.; Roberts, J. M., Modeling heterogeneous ClNO2 formation, chloride availability, and chlorine cycling in Southeast Texas. *Atmospheric Environment* **2010,** *44*, (40), 54765488.

20. Sillman, S.; Logan, J. A.; Wofsy, S. C., The sensitivity of ozone to nitrogen oxides and hydrocarbons in regional ozone episodes. *Journal of Geophysical Research: Atmospheres (1984–2012)* **1990,** *95*, (D2), 1837-1851.

21. Sillman, S., Tropospheric ozone: The debate over control strategies. *Annual Review of Energy and the Environment* **1993,** *18*, (1), 31-56.

22. Environ *User's Guide to the Comprehensive Air Quality Modeling System with Extensions (CAMx), Version 4.10*; 2004.

23. Liang, J.; Jackson, B.; Kaduwela, A., Evaluation of the ability of indicator species ratios to determine the sensitivity of ozone to reductions in emissions of volatile organic compounds and oxides of nitrogen in northern California. *Atmospheric Environment* **2006,** *40*, (27), 5156-5166.

24. McRae, G. J.; Goodin, W. R.; Seinfeld, J. H., Development of a second-generation mathematical model for urban air pollution—I. Model formulation. *Atmospheric Environment (1967)* **1982,** *16*, (4), 679-696.

25. West, J. J., Modeling ozone photochemistry and evaluation of hydrocarbon emissions in the Mexico City metropolitan area. *Journal of Geophysical Research* **2004,** *109*, (D19).

26. Sillman, S.; West, J., Reactive nitrogen in Mexico City and its relation to ozone-precursor sensitivity: results from photochemical models. *Atmospheric Chemistry and Physics* **2009,** *9*, (11), 3477-3489.

27. Liu, X.-H.; Zhang, Y.; Xing, J.; Zhang, Q.; Wang, K.; Streets, D. G.; Jang, C.; Wang, W.-X.; Hao, J.-M., Understanding of regional air pollution over China using CMAQ, part II. Process analysis and sensitivity of ozone and particulate matter to precursor emissions. *Atmospheric Environment* **2010,** *44*, (30), 3719-3727.

28. Wang, X.; Zhang, Y.; Hu, Y.; Zhou, W.; Lu, K.; Zhong, L.; Zeng, L.; Shao, M.; Hu, M.; Russell, A. G., Process analysis and sensitivity study of regional ozone formation over the Pearl River Delta, China, during the PRIDE-PRD2004 campaign using the Community Multiscale Air Quality modeling system. *Atmospheric Chemistry and Physics* **2010,** *10*, (9), 4423-4437.

29. Itahashi, S.; Uno, I.; Kim, S., Seasonal source contributions of tropospheric ozone over East Asia based on CMAQ–HDDM. *Atmospheric Environment* **2013,** *70*, 204-217.

30. Grell, G. A.; Peckham, S. E.; Schmitz, R.; McKeen, S. A.; Frost, G.; Skamarock, W. C.; Eder, B., Fully coupled "online" chemistry within the WRF model. *Atmospheric Environment* **2005,** *39*, (37).

31. Tie, X.; Geng, F.; Guenther, A.; Cao, J.; Greenberg, J.; Zhang, R.; Apel, E.; Li, G.; Weinheimer, A.; Chen, J.; Cai, C., Megacity impacts on regional ozone formation: observations and WRF-Chem modeling for the MIRAGE-Shanghai field campaign. *Atmospheric Chemistry and Physics* **2013,** *13*, (11), 5655-5669.

32. Zhang, L.; Wang, T.; Zhang, Q.; Zheng, J.; Xu, Z.; Lv, M., Potential sources of nitrous acid (HONO) and their impacts on ozone: A WRF-Chem study in a polluted subtropical region. *Journal of Geophysical Research: Atmospheres* **2016,** *121*, (7), 3645-3662.

33. Li, Q.; Zhang, L.; Wang, T.; Tham, Y.; Ahmadov, R.; Xue, L.; Zhang, Q.; Zheng, J., Impacts of heterogeneous uptake of dinitrogen pentoxide and chlorine activation on ozone and reactive nitrogen partitioning: improvement and application of the WRF-Chem model in southern China. *Atmospheric Chemistry and Physics* **2016,** *16*, (23), 14875-14890.

34. Sarwar, G.; Simon, H.; Bhave, P.; Yarwood, G., Examining the impact of heterogeneous nitryl chloride production on air quality across the United States. *Atmospheric Chemistry and Physics* **2012,** *12*, (14), 6455-6473.

35. Sarwar, G.; Roselle, S. J.; Mathur, R.; Appel, W.; Dennis, R. L.; Vogel, B., A comparison of CMAQ HONO predictions with observations from the Northeast Oxidant and Particle Study. *Atmospheric Environment* **2008,** *42*, (23), 5760-5770.

36. Simon, H.; Kimura, Y.; McGaughey, G.; Allen, D. T.; Brown, S. S.; Osthoff, H. D.; Roberts, J. M.; Byun, D.; Lee, D., Modeling the impact of ClNO2 on ozone formation in the Houston area. *Journal of Geophysical Research: Atmospheres (1984–2012)* **2009,** *114*, (D7).

37. Keene, W. C.; Khalil, A. M. K.; Erickson, D. J.; McCulloch, A.; Graedel, T. E.; Lobert, J. M.; Aucott, M. L.; Gong, S.; Harper, D. B.; Kleiman, G.; Midgley, P.; Moore, R. M.; Seuzaret, C.;

455 Sturges, W. T.; Benkovitz, C. M.; Koropalov, V.; Barrie, L. A.; Li, Y., Composite global emissions
456 of reactive chlorine from anthropogenic and natural sources: Reactive Chlorine Emissions
457 Inventory. *Journal of Geophysical Research: Atmospheres (1984–2012)* **1999,** *104*, (D7), 8429-
458 8440.

459 38. Peckham, S. E.; Grell, G.; McKeen, S. A.; Ahmadov, R.; Wong, K. Y.; Barth, M.; Pfister,
460 G.; Wiedinmyer, C.; Fast, J. D.; Gustafson, W. I., WRF-Chem user's guide. **2017**.

461 39. Emmons, L. K.; Walters, S.; Hess, P. G.; Lamarque, J. F.; Pfister, G. G.; Fillmore, D.;
462 Granier, C.; Guenther, A.; Kinnison, D.; Laepple, T.; Orlando, J.; Tie, X.; Tyndall, G.;
463 Wiedinmyer, C.; Baughcum, S. L.; Kloster, S., Description and evaluation of the Model for Ozone
464 and Related chemical Tracers, version 4 (MOZART-4). *Geoscientific Model Development* **2010,**
465 *3*, (1), 43-67.

466 40. Wang, T.; Tham, Y. J.; Xue, L.; Li, Q.; Zha, Q.; Wang, Z.; Poon, S. C.; Dubé, W. P.; Blake,
467 D. R.; Louie, P. K., Observations of nitryl chloride and modeling its source and effect on ozone in
468 the planetary boundary layer of southern China. *Journal of Geophysical Research: Atmospheres*
469 **2016,** *121*, (5), 2476-2489.

470 41. Li, L.; Chen, C.; Huang, C.; Huang, H.; Zhang, G.; Wang, Y.; Chen, M.; Wang, H.; Chen,
471 Y.; Streets, D. G.; Fu, J., Ozone sensitivity analysis with the MM5-CMAQ modeling system for
472 Shanghai. *Journal of Environmental Sciences* **2011,** *23*, (7), 1150-1157.

473 42. Ou, J.; Yuan, Z.; Zheng, J.; Huang, Z.; Shao, M.; Li, Z.; Huang, X.; Guo, H.; Louie, P. K.,
474 Ambient ozone control in a photochemically active region: short-term despiking or long-term
475 attainment? *Environmental science & technology* **2016,** *50*, (11), 5720-5728.

476 43. Liu, Z.; Wang, Y.; Gu, D.; Zhao, C.; Huey, L. G., Summertime photochemistry during
477 CAREBeijing-2007: RO x budgets and O 3 formation. *Atmospheric Chemistry and Physics* **2012,**
478 *12*, (16), 7737-7752.

479 44. Guo, S.; Hu, M.; Zamora, M. L.; Peng, J.; Shang, D.; Zheng, J.; Du, Z.; Wu, Z.; Shao, M.;
480 Zeng, L.; Molina, M. J.; Zhang, R., Elucidating severe urban haze formation in China. *Proceedings*
481 *of the National Academy of Sciences* **2014,** *111*, (49), 17373-17378.

482 45. Pan, Y.; Wang, Y.; Zhang, J.; Liu, Z.; Wang, L.; Tian, S.; Tang, G.; Gao, W.; Ji, D.; Song,
483 T.; Wang, Y., Redefining the importance of nitrate during haze pollution to help optimize an
484 emission control strategy. *Atmospheric Environment* **2016,** *141*, 197-202.

485 46. Li, H.; Zhang, Q.; Zhang, Q.; Chen, C.; Wang, L.; Wei, Z.; Zhou, S.; Parworth, C.; Zheng,
486 B.; Canonaco, F., Wintertime aerosol chemistry and haze evolution in an extremely polluted city
487 of the North China Plain: significant contribution from coal and biomass combustion. *Atmospheric*
488 *Chemistry and Physics* **2017,** *17*, (7), 4751-4768.

489 47. Yang, T.; Sun, Y.; Zhang, W.; Wang, Z.; Liu, X.; Fu, P.; Wang, X., Evolutionary processes
490 and sources of high-nitrate haze episodes over Beijing, Spring. *J Environ Sci (China)* **2017,** *54*,
491 142-151.

492 48. Cohan, D. S.; Hu, Y.; Russell, A. G., Dependence of ozone sensitivity analysis on grid
493 resolution. *Atmospheric Environment* **2006,** *40*, (1), 126-135.

494